EARLY ONLINE RELEASE

This is a preliminary PDF of the author-produced manuscript that has been peer-reviewed and accepted for publication. Since it is being posted so soon after acceptance, it has not yet been copyedited, formatted, or processed by AMS Publications. This preliminary version of the manuscript may be downloaded, distributed, and cited, but please be aware that there will be visual differences and possibly some content differences between this version and the final published version.

A Preliminary Statistical Study of Correlations Between Inflow

Feeder Clouds, Supercell or Multicell Thunderstorms, and

Severe Weather

by

Rebecca J. Mazur[1]
NOAA/National Weather Service
Cheyenne, WY

John F. Weaver
NOAA/NESDIS/RAMM Team
Cooperative Institute for Research in the Atmosphere, CIRA
Colorado State University

Thomas H. Vonder Haar
Professor, Department of Atmospheric Science
Colorado State University
Fort Collins, CO 80523

---

[1] Corresponding Author Address; 1301 Airport Parkway, Cheyenne WY, 82001

Abstract

This study examines the relationship between severe weather and organized lines of cumulus towers, called feeder clouds, which form in the inflow region of supercell and multicell thunderstorms. Using Geostationary Operational Environmental Satellite (GOES) imagery, correlations between the occurrence of feeder clouds and severe weather reports are explored. Output from the WSR-88D Mesocyclone Detection Algorithm (MDA) is also assessed for a subset of the satellite case days. Statistics from the satellite and radar data sets are assembled to estimate not only the effectiveness of feeder cloud signatures as sole predictors of severe weather, but also the potential utility of combining feeder cloud analysis with the radar's MDA output.

Results from this study suggest that the formation of feeder clouds as seen on visible satellite imagery is often followed by the occurrence of severe weather in a storm. The study finds that feeder cloud signatures by themselves have low skill in predicting severe weather. However, if feeder clouds *are* observed in a storm, there is a 77% chance that severe weather will occur within 30 min of the observation. For the cases considered, the MDA turns out to be the more effective predictor of severe weather. However, results show that combined predictions (feeder clouds plus mesocyclones) outperform both feeder cloud signatures and the MDA as separate predictors by ~10-20%. Thus, the presence of feeder clouds as observed on visible imagery is a useful adjunct to the MDA in diagnosing a storm's potential for producing severe weather.

1. Introduction

This study examines the relationship between severe weather and organized lines of cumulus towers that form in the inflow region of strong thunderstorms (Weaver et al. 1994; Weaver and Lindsey 2004). These cumulus lines have been labeled inflow feeder clouds, or simply feeder clouds. Fig. 1 shows the evolution of feeder clouds (indicated by the white arrows) in a storm over a period of 15 minutes. Feeder clouds are situated in the warm sector downstream of the main updraft, which on satellite imagery is viewed as the overshooting top (OST). These cloud features are oriented roughly 45°- 90° to the storm motion, and are a quasi-steady feature relative to the storm. They typically join the updraft on its eastern or southeastern edge (Weaver et al. 1994). The distinguishing characteristic of feeder clouds is the noticeable convergence toward the main updraft, or OST.

Feeder clouds are similar in appearance to horizontal convective rolls; often as alternating lines of clouds/no clouds collocated with regions of upward and downward motion, respectively (described in Weckwerth et al. 1997, 1999). However, feeder clouds are shorter, more compact clouds lines that converge toward the updraft, while HCR's are typically longer and are generally parallel to one another. Some feeder cloud clusters lack a distinct clearing between lines, but the convergence toward the updraft is obvious (see Figs. 3 and 4 from Weaver and Purdom 1995). It is unclear at this point whether feeder clouds are a subset of environmental HCR's under the strong influence of the main updraft of a storm, or if they form as a consequence of increased shear in the inflow region due to the acceleration provided by the updraft.

Prediction of severe thunderstorms is complex, since many interacting weather features – from the mesoscale to the synoptic – help create an environment conducive to their formation

and intensification (Klemp et al. 1981; Lemon and Doswell 1979; Purdom 1982; Johns and Doswell 1992; Wilson et al. 1992; Weaver et al. 1994; Weaver and Purdom 1995; Weckwerth et al. 1996; Atkins et al. 1998; Weckwerth 2000). Difficulties notwithstanding, it is essential to be able to make accurate and timely forecasts of these storms in order to save lives and mitigate property losses. Satellite imagery can help the forecaster in this process by providing indications of where a thunderstorm or group of thunderstorms might form, identifying factors affecting storm evolution, furnishing clues regarding severe weather potential, and hinting as to how the storms(s) might propagate (Adler and Fenn 1979; McCann 1983; Scofield and Purdom 1986; Heymsfield and Blackmer 1988; Bunkers et al. 2000; Weaver et al. 2002). In particular, storm scale cloud features on the order of 1-10 km are resolved on 1 km visible satellite imagery and have been shown to be influential in storm evolution (Lemon 1976; Weaver et al. 1994; Weaver and Purdom 1995; Weaver and Lindsey 2004). Feeder clouds fall into this category.

The significance of feeder clouds has not been addressed extensively in the literature, nor has a correlation been established between the formation of these features and the occurrence of severe weather[2]. However, Weaver and Lindsey (2004) suggest that feeder clouds may often be a signal of rapid storm intensification in supercell thunderstorms and that severe weather may be imminent. The present study addresses this suggested relationship by determining whether the formation of feeder clouds is common to severe supercell and multicell thunderstorms, and whether these features might provide new and useful information regarding severe potential to severe storm forecasters. This is done by developing correlations between the presence of feeder clouds in a storm as viewed on visible satellite imagery and the occurrence of severe weather. An assessment is presented of the predictive skill of feeder cloud signatures by calculating the

---

[2] Severe weather is defined by the National Weather Service, and in this study, as hail ≥ 0.75 in. in diameter, winds ≥ 58mph (50 kt), and/or tornadoes.

probability of detection (POD), false alarm rate (FAR), and critical success index (CSI) as defined by Donaldson et al. (1975) for the various cases. Next, the radar-based Mesocyclone Detection Algorithm (MDA, Stumpf et al. 1998) is run for a subset of the selected cases as a comparison data set. Stumpf et al. (1998) found that 90% of storms in which mesocyclones were detected produced severe weather. The MDA was designed to detect these mesoscale circulations and to alert the forecaster in real time. Since the MDA is currently used in severe weather warning operations, comparing feeder cloud signatures to MDA detections as predictors of severe weather seems constructive. Additionally, relating the formation of feeder cloud signatures to mesocyclone formation might lend support to the notion that the formation of feeder clouds is related to the intensification of the storm.

2. Data sources

For this study, feeder clouds were identified using the 1 km resolution visible wavelength channel from the Geostationary Operational Environmental Satellite (GOES) imager, exclusively. At present, we are simply trying to identify feeder clouds in as accurate and timely a manner as possible, and the high resolution visible channel is the best way to do so. When GOES-R comes online in a few years, the IR channels will have much better resolution, and those data can also be used for expanded statistical studies, or in forecasting applications.

Frequent interval imagery is available using either the normal scanning schedule, or rapid-scan operation (RSO) scheduling. Normal scanning operations collects images every 15 minutes except for four-times daily, when a full-disk, 30 min scan is scheduled. When requested, RSO images can be taken over the US at intervals that vary to include 5, 7, 10, and 12 minutes (Kidder and Vonder Haar 1995). However, this schedule is also interrupted four times

daily for the full-disk scan. RSO imagery is useful during severe weather situations when the environment can change rapidly. Animated loops can be used to highlight cloud features that are evolving or persistent over time, such as growing storms, overshooting tops, mesoscale boundaries, etc.

For this study, GOES visible imagery was analyzed from 24 days on which severe weather occurred. Severe weather days were chosen in a variety of regions of the contiguous US during each season. The satellite data included both RSO and normal scanning operations, depending on what was available. A McIDAS (Lazzara et al. 1999) display system served as the visualization tool for displaying the data.

As mentioned previously, feeder cloud signatures were compared to MDA detections derived from WSR-88D data. The MDA was analyzed for a subset of 15 of the 24 satellite case days to identify storms having mesocyclones. Traditionally, a storm having a mesocyclone is considered a supercell thunderstorm (Moller et. al 1994). By comparing feeder clouds to mesocyclone detections, we are not however implying feeder clouds are solely a feature of supercells. The purpose was to use the MDA as a comparison dataset for assessing predictive skill, and not an identifier of storm type. There are several reasons that only a portion of the cases were included in the radar analysis. During the data acquisition process, a number of cases did not have archived Level II radar data available for the appropriate radar site. Additionally, processing radar data with the ORPG[3] was resource intensive and required more time than was allowed for this project. Lastly, since radar data were utilized as a comparative data set only, a one-to-one match was not critical.

The MDA output is produced by an automated radar process which is used in National Weather Service (NWS) operational forecasting. It identifies circulations in storms using the

---

[3] Open Radar Product Generator – a radar product generation software package

WSR-88D radial velocity – a function that measures integrated particle velocities in a volume scan toward and away from the radar and is used to detect areas of high wind and rotation in a storm (Burgess 1976; Brown and Wood 1991; Moller 2001; Stumpf et al. 1998; Wood et al. 1996). The algorithm identifies which circulations meet mesocyclone criteria, thereby marking which cells might represent a severe weather threat. Characteristics of a mesocyclone such as strength and size, which is not obvious on velocity data, can be sampled using the MDA. Not all thunderstorms that produce severe weather have mesocyclones, but those storms with mesocyclones have a significant chance of producing severe weather and will likely be highlighted by the MDA.

The method used to verify severe weather follows that used by a number of severe storms research projects (Carey et al. 2003; Jones et al. 2004; Stumpf et al. 1998; Trapp et al. 2005). Severe storm reports taken from the National Climatic Data Center (NCDC) Storm Events database were compared in time and space to storms observed on visible satellite imagery. This database contains point severe weather reports, so, as suggested by Witt et al. (1998), a time window was selected (similar to that of Jones et al. 2004, Stumpf et al. 1998, and Trapp et al. 2005) to extend the utility of a single point report over a longer period of time. Employing a time window also helped to minimize errors due to non-meteorological factors, such as inaccurately reported times. Storms that propagate over non-populated areas create another verification concern, namely an increased likelihood that severe weather will not be reported. Under-reporting creates inaccurate false-alarm signals in verifying severe weather for those storms (Witt et al. 1998). No attempt was made to adjust for this effect.

3.   Case Study from 8 May 2003

This section provides an example of the evolution of feeder clouds in a supercell thunderstorm coincident with other storm features viewed on satellite and radar imagery. Specifically, features such as the overshooting top (OST, Adler and Mack 1986), flanking lines (Lemon 1976), and mesocyclones will be discussed in relation with the occurrence of feeder clouds (Fig. 2) since these features are known to be associated with severe storms. The purpose here is to illustrate how feeder clouds relate to storm intensification by comparing their evolution with other well known storm features.

A supercell formed over central Oklahoma on the afternoon of 8 May 2003. The first towering cumulus clouds were observed around 2015 UTC on a north-south oriented dryline. As the towers organized and moved eastward, the storm rapidly intensified, and storm splitting could be seen on radar beginning at 2116 UTC (not shown). By 2125 UTC, a large OST had formed and a mesocyclone was detected by the KTLX Doppler radar (not shown). The 2132 UTC visible satellite image (Fig. 3A) shows a large OST with an anvil spreading rapidly from the updraft. This anvil expansion suggests that an intense updraft was developing. An inflow notch can be seen at the southwestern end of the storm complex, even though no mesocyclone was detected by the MDA in the updraft region (Fig. 3D). The mesocyclone identified on the north flank was associated with the smaller storm core north of the supercell.

At 2132 UTC (Fig. 3A), the supercell's inflow region is covered by a high cirrus deck. No feeder clouds can be seen in the storm's updraft region at this time, though a well-defined flanking line had formed (line of enhanced cloud extending southwest from the storm, denoted by the yellow arrow in Fig. 3A). There are HCR's evident south and east of the storm (denoted by black arrows), but none connect with the updraft and do not converge toward the storm.

7

However, the storm is moving toward these HCR's, and so one might expect an enhancement of these features as the storm traverses eastward.

By 2145 UTC (Fig. 3B), the anvil has expanded and the OST has decreased somewhat in size. Note also that the first feeder clouds (i.e., the enhanced lower-level cumulus on the southwestern side, denoted by cyan arrows) have begun to show through the cirrus cover, coincident with the smaller, but persistent OST. These feeder clouds look similar to the environmental HCR's on the south and east flanks of the storm, but show convergence toward the updraft. This convergence is the distinguishing factor between the environmental HCR's and feeder clouds. The example described here lends support to the notion that some feeder clouds are enhanced HCR's in the near storm environment, however nothing definitive can be stated at this time. Coincidentally, a mesocyclone was identified by the KTLX radar from 2136-2150 UTC (seen at 2145 UTC in Fig. 3E) and a hook echo was persistent in the reflectivity field throughout this time period, beginning at 2131 UTC (Fig. 3D).

The feeder clouds had grown in size and number by 2202 UTC (Fig. 3C) as the updraft continued to produce a single, well-defined overshooting top. The feeder clouds evolved from distinct low level lines into a large, compacted region of cloud lines with increased convergence toward the updraft. On radar, the hook had increased in size with reflectivities of 55 dBz at 2200 UTC (Fig. 3F) coincident with a persistent mesocyclone detection. These factors indicate rotation in the storm updraft was strong at this time.

Following the enhancement of the feeder clouds on satellite and the hook echo and mesocyclone detection on radar, large hail was reported in the storm at 2155 UTC and 2158 UTC and an F0 tornado was reported at 2200 UTC. The storm produced an F4 tornado 15 minutes later.

This example illustrates the unique visual characteristics of feeder clouds. In this case, feeder cloud development was associated with storm intensification; forming shortly after the enhancement of the OST and flanking lines on satellite imagery, and coincident with the rapid organization of the radar reflectivity field. Also, feeder cloud development occurred prior to the onset of severe weather and was seen on satellite imagery at least ten minutes before the first report was received.

4. Sampling and testing methodology

a. Thunderstorm Selection

Thunderstorms were chosen using GOES visible imagery from 24 days on which severe weather occurred. The general area from which storms were chosen had known occurrences of severe weather, but the individual storms were selected prior to any in-depth analysis of severe reports to include both severe and non-severe storms. This was necessary to determine whether feeder clouds were unique to severe thunderstorms. A storm was selected for satellite analysis if the inflow region could be distinguished for a minimum of three RSO scans (~15 minutes which allowed time for storm scale features to evolve) or on two images taken in normal scanning mode. In order to evaluate the utility of feeder cloud signatures in severe weather forecasting, it was important to choose storms from which the inflow region was discernible to know whether or not feeder clouds had formed.

It was further required that the selected storm be relatively long-lived (i.e., long enough to meet the testing criteria) and easy to track visually. Persistent storm features observed on satellite imagery such as flanking lines or OSTs were used to make this determination, although each feature was not seen in every storm. Feeder clouds were not one of these features utilized,

since they were the element under investigation. Based on these criteria, 130 storms including

supercells and multicells were chosen for analysis. Table 1 lists the date of each case, the

number of storms analyzed for each case, and general location from which storms were chosen.

b. Feeder Cloud, Mesocyclone, and Severe Weather Identification.

Once a storm was chosen, it was examined over a period of analysis for the occurrence of

feeder clouds and mesocyclones. The period of analysis began with the first scan in which the

inflow region near the updraft was in view, and ended when it could no longer be distinguished.

Instances that would prevent a clear view of the inflow region and any potential feeder clouds

include nightfall, a broad anvil from the parent storm or a nearby storm, another storm situated in

the satellite's direct line of site, or a new storm forming in the inflow region.

The OST was used as an updraft reference feature to help determine whether the anvil of

a given storm allowed a clear view of the inflow region. It was also used to track the storm,

since the OST propagates along the path of updraft regeneration. Finally, the OST was used as a

first indication of a strong thunderstorm, since an OST that is long-lived and large in vertical and

horizontal extent is indicative of a strong updraft (Rauber et al. 2002). Since the main purpose of

this study is to analyze feeder clouds on satellite data, it's only natural to use satellite imagery to

track and diagnose strength of a storm. Using radar data to diagnose storm strength is more a

supplement instead of a main focus. The time of each satellite scan, characteristics of the OST

and flanking line (if present), and whether feeder clouds occurred were then tabulated for each

storm.

A similar methodology was used for recording mesocyclone detections from the MDA.

Table 2 lists the cases available for the radar comparison. Reflectivity cores were paired in time

and space with the storms chosen for satellite analysis using the latitude/longitude readout in

McIDAS. MDA output for each volume scan was then analyzed to determine which detections met the criteria to be considered a mesocyclone. Similar to Trapp et al. (2005), detections were classified as mesocyclones if a circulation of rank-5[4] or greater was; 1) detected at or below 5 km above radar level, 2) observed throughout a vertical depth $\geq$ 3 km, and 3) persisted for a period longer than one radar volume scan (5 or 6 min). For further details see Stumpf et al. (1998) and Trapp et al. (2005). If more than one detection met these criteria in a storm, then the strongest detection was used for statistical analysis. The time of each radar scan and whether mesocyclones were detected was logged coincident with data compiled from the analysis of satellite imagery.

Once a storm was examined for the presence of feeder clouds and mesocyclones, storm reports were analyzed to determine whether it was severe. Reports were plotted on the visible imagery scan that matched closest in time with the report using the city locator or latitude/longitude feature of McIDAS. For a report to be associated with a storm, its location had to be in the storm core within 50 km of the parallax corrected OST (Heymsfield et al. 1983). Occasionally, multiple storms occurred under an anvil even though only one OST was visible. Placing a distance constraint on the report relative to the parallax corrected OST was necessary to minimize the chance that a report was associated with a different storm core under the same anvil. The time of the report that matched with a particular storm was recorded coincident with information from satellite and radar imagery for later analysis.

Finally, observations from radar and satellite data were combined to evaluate whether using information from both sources might improve the short term prediction of severe weather. The idea was to combine the two data sources to be used as one source, and evaluate whether the

---

[4] Strength Rank 5 circulation is an MDA shear segment with a velocity difference of 30-35 ms^{-1} and shear of 6-6.74 ms^{-1}km^{-1}

combination of data would be better or worse than using either alone. Typically, when utilizing two different data sources for analysis, one would use instances where the two data sources occurred at the same instance in time, or within a short time interval. Since there are typically more radar data available versus satellite data, the combined dataset of satellite and radar data have periods when only radar data is available. For the purpose of this study, we considered the combined dataset to include the pairing of satellite and radar together when they occurred within 3 minutes of each other, and for radar alone at times when there was no matching satellite imagery. The latter occurred only occasionally. This methodology allowed for all available radar and satellite scans to be included in the statistical analysis, since all the data would likely be available in real-time operations. Also, combining the satellite and radar scans in this manner made the scoring procedure synonymous to scoring satellite and radar data separately. It follows then that a combined scan with either feeder cloud signatures and/or mesocyclones was called a "combined detection." Data collected from combined scans were logged coincident with information from the satellite and radar analysis.

c. Classification and Scoring Methods.

As previously noted, the method employed for quantifying the relationship between the presence of feeder clouds, mesocyclone detections, and severe weather utilized a time window, rather than the single time. For this study, a time window of -30 min to +10 min around each severe weather report was chosen. The 30 min advance period allowed for at least two visible scans to be examined with sufficient lead time to predict the severe weather event. The 10 min lag allowed for minor timing errors in storm reports. Furthermore, if a report happened to fall at the end of one of the longer 30 min breaks in visible imagery, it was not used for scoring

purposes since feeder clouds have been observed by the authors to occur on time scales much less than 30 min.

Table 3 shows the generalized contingency table template used to classify each visible, radar, and combined scan for statistical analysis in this study. In the case of satellite imagery, the "algorithm" is simply the presence or absence of feeder clouds on a visible scan. For the radar data, the "algorithm" is the presence or absence of an MDA-detected mesocyclone. Each scan in which feeder clouds (or mesocyclones) were observed was classified as a positive, or "yes" algorithm prediction. All scans in which feeder clouds (or mesocyclones) were not observed were considered negative, or "no" predictions. Remembering that the time window around a severe storm report is -30 min to +10 min, all scans that fell within this time window were considered a "yes" event, and thus were associated in time with a severe weather event. Similarly, all scans that fell outside the time window were considered a "no" event, and therefore were not associated with severe weather.

There were four possible outcomes to consider; a) a "Hit," [severe weather was predicted and did occur], b) a "False Alarm" (FA), [severe weather predicted, but did not occur], c) a "Miss," [no severe weather was predicted, but it did occur], and d) a correct "no" prediction (null), [no severe weather was predicted, and none occurred].

After all satellite, radar, and combined scans were classified and tallied, the POD, FAR, and CSI were calculated using the following relationships (after Donaldson et al. 1975):

$$POD = a / (a + c) \quad (1)$$

$$FAR = b / (a + b) \quad (2)$$

$$CSI = a / (a + b + c) \quad (3)$$

The POD, FAR, and CSI were used to evaluate each storm feature as a potential predictor of severe weather, separately and together, to see which has the most predictive skill. Additionally, these scores were useful in quantitatively identifying the relationship between the occurrence of feeder clouds and severe weather. Results of the analysis are discussed in the next section.

5. Results

This section presents results from the analysis described in the previous section. Classification results and skill scores are discussed for feeder cloud signatures, MDA detections, and the combined prediction by both signatures.

a. Classification and Scoring Results for Feeder Cloud Signatures.

Results for classifying feeder cloud signatures as severe weather predictors are summarized in Fig. 4. Of the 130 storms chosen for this study, a total of 1238 visible scans were classified using the criteria described in section 4c. There were a total of 269 hits, 81 false alarms, 497 misses, and 391 nulls. From these results, it is clear that a considerable number of severe weather events were not predicted by feeder cloud signatures, since 40.1% of all visible images were classified as missed predictions and only 21.7% were hits. This result implies that feeder clouds are not a necessary condition for severe weather to occur in a storm. Combining the misses and null categories, we see that 71.7% of all satellite scans did not have detectable feeder clouds. This further implies that feeder clouds are not commonly observed features of thunderstorms in this study.

The POD, FAR, and CSI were next computed using equations (1) - (3) for the feeder clouds signatures. As seen in Fig. 5, feeder cloud signatures score relatively low in overall prediction of severe weather (POD = 35.1%, CSI = 31.2%). The low POD and CSI were largely

14

influenced by both the difficulty in viewing the updraft region at some times, and the fact that feeder clouds may not be present in a large number of severe storms. If one were to expand upon the thunderstorm population in this study to include all storms, it is likely the POD and CSI would be worse due to the fact that feeder clouds are likely hidden from view in a number of storms and therefore more misses would be tallied. Clearly, waiting to see feeder cloud signatures on visible imagery to diagnose severity would not provide positive results. However, the low FAR (23.1%) suggests that if feeder clouds *are* observed in a storm, there is a good chance (76.9%) that severe weather will occur within 30 min of that observation. In those cases, the storm has a high probability of producing severe weather shortly after the occurrence of feeder clouds.

Regarding severe weather forecasting, results here suggest that observations of feeder clouds can be used to presume a storm's potential for producing severe weather within 30 min, more than 75% of the time. This can give a forecaster further confidence in warning for a storm when other environmental parameters are favorable for severe weather, in addition to circumstances when the radar is out of operations.

b. Results for the Mesocyclone Detection Algorithm Subset.

Predictions by the MDA are also summarized in Fig. 4. A subset of radar data for 15 of the satellite case dates was available for MDA analysis. From this subset, 1503 radar volume scans were classified using the criteria described in section four. The classification yielded 481 hits, 80 false alarms, 593 misses, and 349 null predictions. As in the case of feeder cloud signatures alone, there were a high percentage of misses (39.5%) indicating that a mesocyclone is not necessary for a storm to produce severe weather. Combining misses with nulls we see that

62.7% of all radar scans did not have mesocyclones, implying that mesocyclones are not common to all storms in this study.

The skill scores for the MDA data are shown in Fig. 5. The Doppler radar algorithm clearly outperforms feeder cloud signatures, since the POD (44.8%) and CSI (41.7%) are considerably higher. Also, the FAR (14.3%) is lower, suggesting that if a mesocyclone is detected in a storm, there is a higher likelihood (85.7%) compared to feeder clouds (76.9%) that severe weather will occur within 30 min. These results suggest that the MDA, overall, has more skill in predicting severe weather. The findings for the MDA are similar to Stumpf et al. (1998) and Jones et al. (2004), although a direct comparison is difficult to make. In those studies, only certain attributes of mesocyclone size and strength (computed by the MDA) were scored against severe weather, with an emphasis on tornadoes. Here, we essentially scored all types of severe weather against the entire set of MDA attributes. Still, the results are convincingly similar.

One reason that the MDA may have outperformed feeder cloud signatures at predicting severe weather – apart from the obvious fact that the Doppler radar can look directly into the storm – is that more radar volume scans were available for this analysis (every 5-6 min) when compared to the available visible imagery scans (taken at intervals of 5, 7, 10, 12, 15 and 30 minutes). This is a typical scheduling difference. Also, a radar can sample the storm with limited obstruction whereas feeder clouds may be obstructed from view by the satellite more often than is known. One might also presume that more false alarms would occur, but that was not the case.

c. *Results for Combined Feeder Cloud and Mesocyclone Predictions.*

Data from a subset of the satellite cases were merged with the corresponding 15 radar cases to classify and score combined detections. As described in section four, combined scans

16

are defined as satellite and radar scans that occur at the same time or within three minutes of one another. Additional combined scans are tallied for each unmatched radar scan. The presence of feeder clouds and/or mesocyclones on a combined scan is called a combined detection. Based on these criteria, a total of 1511 combined scans were tabulated. The results are summarized in Fig. 4.

The classification yielded 599 hits, 122 FAs, 490 misses, and 300 nulls. For this classification, 47.7% of combined scans saw mesocyclone detections and/or feeder cloud signatures (hits plus false alarms) meaning that at least one of these features was observed in nearly half of the visible and/or radar scans examined in this study. The percentage of hits (39.6%) is higher, meaning that the combined detections correctly predicted more severe weather events than either the occurrence of feeder clouds or mesocyclone detections alone. These preliminary results, based on a small data set, are encouraging. However, a 39.6% hit ratio means that numerous severe weather events were still not predicted by either sensor. It is clear that a storm can produce severe weather without the presence of either detectable feeder clouds or mesocyclones.

On the whole, combined detections outperformed both feeder cloud signatures and mesocyclone detections as sole predictors of severe weather (Fig. 5). The low FAR (16.9%) indicates that when feeder clouds, mesocyclone detections, or both storm features are observed on satellite and/or radar, there is a ~83% likelihood that severe weather will occur within 30 min. The FAR for the combined detections is 2.6% worse than that for MDA detections alone, and 6.2% better than that calculated for feeder cloud signatures. However, all three methods have impressively low FAR's.

17

To test whether these results are statistically significant, a simple two-sample hypothesis test was run on the MDA results alone versus those of the combined detections. The test shows that there is sufficient evidence to conclude that both the POD and CSI for the combined data set is significantly higher than those for the satellite or MDA alone, at a 1% level of significance. Since the MDA is currently utilized during warning operations as a predictor of severe weather, it is suggested that a quick check for feeder cloud signatures on visible satellite imagery may be a useful adjunct when diagnosing a storm's potential to produce severe weather. The hypothesis test for FAR does not allow us to conclude that the MDA is significantly lower than the combined data set at a 1% level of significance. However, that conclusion survives at a 2.2% level.

d. Summary of Statistical Results.

The results from this analysis indicate that combined detections have the most skill as short-term predictors of severe weather in terms of POD and CSI. In terms of FAR, the MDA is slightly better by 2.6%, but the POD and CSI for combined detections are ~10-20% higher than both feeder cloud signatures and MDA detections. Therefore, by using observations of feeder cloud signatures in combination with mesocyclone detections from the MDA, the likelihood that severe weather will be accurately predicted is significantly better than by using either feature alone. Additionally, the low FAR for feeder cloud signatures suggests there is a relationship between the formation of these features and the onset of severe weather.

6. Conclusions and suggestions for future research

a. Conclusions.

Based on observations of feeder clouds, severe weather, and mesocyclone detections from the MDA in supercell and multicell thunderstorms, this study has established a relationship between the occurrence of feeder clouds and severe weather. It has been shown that:

1) Feeder cloud development is an indication that a storm may produce severe weather. As demonstrated for a supercell thunderstorm in section three, the OST and flanking line became enhanced on satellite imagery, and the radar reflectivity core intensified just prior to the formation of feeder clouds. Mesocyclone detections from the MDA were observed during this intensification phase as well. Following the enhancement of these features, severe weather occurred. We were not able to establish whether feeder clouds contribute in some way to storm intensification, or simply form in reaction to this intensification. Further investigation with field observations and modeling efforts would be needed to address this query.

2) In general, feeder clouds were observed in only 28.3% of the visible satellite scans analyzed for this study. Therefore, it seems reasonable to assert that feeder clouds are not common to all intense thunderstorms. One thing to note though is that the number of storms analyzed in this study was diminished from the overall population of storms that occurred on each day due to the criteria that the inflow region had to be discernable for a certain time period to qualify for analysis. Therefore, the overall number of storms with feeder clouds could potentially be higher, but factors such as the anvil overshadowing the inflow region and nightfall would make any development of feeder clouds impossible to see.

3)   Adding information about the presence of feeder clouds to information gleaned from the

Doppler radar during severe weather operations can improve forecast confidence. The

FAR (23.1%) suggests that if feeder clouds are observed in a storm, there is a 76.9%

chance that severe weather will occur within 30 min. In comparison to feeder cloud

signatures, the skill of the MDA at predicting severe weather (POD = 44.8%, CSI =

41.7%, and FAR = 14.3%) was measurably greater.   Combining information from

satellite and radar, the low FAR (16.9%) for combined detections indicates that when

feeder clouds, mesocyclone detections, or both are observed on satellite and/or radar,

there is an 83.1% likelihood that severe weather will occur within 30 min. These

results show that feeder cloud signatures are a comparable algorithm to the MDA,

however they are not recommended to use as a standalone algorithm when radar data

is available.

Ultimately, the presence of feeder clouds in a developing thunderstorm should provide

valuable and welcome information in the warning decision making process, particularly in

environments where severe thunderstorms are anticipated. Feeder cloud signatures observed in a

storm during the warning decision making process should allow a forecaster more confidence

when issuing a warning, especially when radar and other observational data support a severe

storm. Additionally, the presence of feeder cloud signatures may convince a forecaster to warn

when the radar is out of operation or if a storm is some distance from the radar and is poorly

sample.   For now, this statement is only true during daytime hours. That will change when

future GOES satellites display infrared data at higher resolutions.

b. Suggestions for Future Work.

In many ways, this study asks more questions than it answers. Obviously, it would be interesting to expand the number of satellite and corresponding radar cases to generate a greater population of thunderstorms for statistical analysis, as well as to include more storms in mountainous and coastal regions which were not well represented in this study. In future studies, with larger data bases, it would be interesting to calculate the POD, FAR, and CSI for the feeder cloud signatures according to severe weather type and strength as well. The authors felt that the population of severe thunderstorms in this analysis was not large enough to calculate reliable statistics according to severe weather type. Ultimately, this information would be most useful in operations to improve a forecaster's confidence in determining greatest threat according to severe weather type.

This study utilized the Storm Events Database as the primary record from which severe weather reports were retrieved. As mentioned in section two, this database has a number of shortcomings, though techniques were employed to lessen any errors associated with time and location. Other available databases were not fully utilized in this study – ones that might provide additional information to further minimize reporting errors. One useful addition would be observational reporting logs maintained during special field programs. Including other databases with Storm Events might help increase the accuracy of the "ground truth" used to reach conclusions.

c. Suggestions for Correlating Feeder Clouds with Storm Intensification.

A correlation between the formation of feeder clouds and thunderstorm intensification was suggested by this study. However, this correlation does not address how and why feeder clouds might evolve in such situations. Future work should include taking observations of the

cloud top temperatures to identify changes in the updraft intensity in relation to the formation of feeder clouds. Relatively colder cloud top temperatures are associated with the overshooting top and are prominent features in severe thunderstorm anvils (Heymsfield and Blackmer 1988). By identifying changes in the coldest temperatures using enhanced IR imagery, changes in updraft intensity can be inferred. Adding information from other satellite channels could provide another straightforward means of judging whether feeder clouds are always associated with rapidly intensifying thunderstorms. In the future, GOES-R will provide higher resolution to improve the identification of feeder clouds during nighttime hours.

Before one truly understands the relationship between feeder clouds and storm intensification, one must be aware of why and how feeder clouds form in a thunderstorm. Field research efforts should be the next step. As suggested by Weaver and Lindsey (2004), these efforts might include 1) pressure measurements southeast of the wall cloud (i.e., east of the flanking line) to document possible correlations between inflow cloud development and updraft intensification, 2) wind and pressure measurements to the west of the main precipitation core to document relationships between the developing rear-flank downdraft and multiple cloud lines, and 3) cloud photography and/or videography, from the middle distance (i.e., 10-30 km), both east and west, of a storm to record how these features develop in real time. Such in-situ observations would help increase our understanding of both updraft and feeder cloud evolution in a thunderstorm from a ground-based perspective.

Lastly, if high resolution numerical models are able to reproduce feeder clouds, the output might be useful in diagnosing the mechanisms that lead to their formation in relation to storm intensification. Feeder clouds are observed to have structures similar to that of horizontal convective rolls and, thus, may be reproducible in models. One idea is that feeder clouds may be

22

forming in an environment in which HCR's are likely. Do the HCR's become enhanced as the environment is influenced by the storm-relative low pressure region (Rotunno and Klemp 1982) on the forward right flank of the supercell? HCR's and associated feeder clouds could also form in the inflow environment as a *response* to storm dynamics. By simulating thunderstorms with initial conditions that are conducive to feeder cloud development, we might be able to discover whether feeder clouds are solely a response to rapid intensification of a storm, or if their underlying structure similar to that of HCR's somehow contributes to storm intensification. Combining field observations with high resolution model analysis seems the next logical step toward understanding these storm features.

7. Acknowledgments

8. References

Adler, R. F. and D. D. Fenn, 1979: Thunderstorm intensity as determined from satellite data. *J. Appl. Sci,* **18,** 502-517.

___ and R. A. Mack, 1986: Thunderstorm cloud top dynamics as inferred from satellite observations and a cloud top parcel model. *J. Atmos. Sci.* **43,** 1945-1960.

Atkins, N. T., R. M. Wakimoto, and C. L. Ziegler, 1998: Observations of Finescale Structure of a dryline during VORTEX 95. *Mon. Wea. Rev.,* **126,** 525-550.

Brown, R. A. and V. T. Wood, 1991: On the interpretation of single-Doppler velocity patterns within severe thunderstorms. *Wea. Forecasting,* **6,** 32-48.

Bunkers, M. J., B. A. Klimowski, J.W. Zeitler, R. L. Thompson, and M. L. Weisman, 2000: Predicting supercell motion using a new hodograph technique. *Wea. Forecasting*, **17**, 845-855.

Burgess, D. W., 1976: Single-Doppler radar vortex recognition. Part I: Mesoscale signatures. Preprints, *17th Conf. on Radar Meteorology*, Seattle, WA, Amer.   Meteor. Soc., 97-103.

Carey, L. D., S. A. Rutledge, and W. A. Petersen, 2003: The relationship between severe storm reports and cloud-to-ground lightning polarity in the contiguous United States from 1989 to 1998. *Mon. Wea. Rev.,* **131,** 1211-1228.

Donaldson, R. J., R. M. Dyer and M. J. Kraus, 1975: An objective evaluation of techniques for predicting severe weather elements. Preprints, *9th Conf. On Severe Loc. Storms*, Boston, MA, Amer. Meteor. Soc., 321-326.

Heymsfield, G. M., K. K. Ghosh, and L. C. Chen, 1983: An interactive system for compositing digital radar and satellite data. *J. Appl. Sci,* **22,** 705-713.

___ and R. H. Blackmer, Jr., 1988: Satellite-observed characteristics of Midwest severe thunderstorm anvils. *Mon. Wea. Rev.,* **116,** 2200-2224.

Johns, R. H. and C. A. Doswell III, 1992: Severe local storm forecasting. *Wea. Forecasting,* **7,** 588-612.

Jones, I. A., K. M. McGrath, and J. T. Snow, 2004: Association between NSSL Mesocyclone Detection Algorithm-Detected vortices and tornadoes. *Wea. Forecasting,* **19,** 872-890.

Kidder, S. Q. and T. H. Vonder Haar, 1995: *Satellite Meteorology: An Introduction.* Academic Press, 466 pp.

Klemp, J. B., R. B. Wilhelmson, and P. S. Ray, 1981: Observed and numerically simulated structure of a mature supercell thunderstorm. *J. Atmos. Sci.,* **38,** 1558-1580.

Lazzara, M. A., J. M. Benson, R. J. Fox, D. J. Laitsch, J. P. Rueden, D. A. Santek, D. M. Wade, T. M. Whittaker and J. T. Young, 1999: The Man computer Interactive Data Access System: 25 years of interactive processing. *Bull. Amer. Meteor. Soc.*, 80, 271-284.

Lemon, L. R., 1976: The flanking line, a severe thunderstorm intensification source. *J. Atmos. Sci,* **33,** 686-694.

___ and C. A. Doswell, III, 1979: Severe thunderstorm evolution and mesocyclone structure as related to tornado genesis. *Mon. Wea. Rev.,* **107,** 1184-1197.

McCann, D. W., 1983: The enhanced-V: A satellite observable severe storm signature. *Mon. Wea. Rev.,* **111,** 887-894.

Moller, A. R., C. A. Doswell, III, M. P. Foster, and G. R. Woodall, 1994: The operational recognition of supercell thunderstorm environments and storm structures. *Wea. Forecasting,* **9,** 327–347

___, 2001: Severe local storms forecasting. *Severe Convective Storms, Meteor. Monogr.,* No. 50 Amer. Meteor. Soc., 433-480.

Purdom, J. F. W., 1982: Subjective interpretation of geostationary satellite data for nowcasting. *Nowcasting*, K.A. Browning, ed., New York, Academic Press, 256pp.

Rauber, R. M., J. E. Walsh, and D. J. Charlevoix, 2002: *Severe and Hazardous Weather.* Kendhall/Hunt Publishing Company, 616 pp.

Rotunno, R. and J. B. Klemp, 1982: The influence of the shear-induced pressure gradient on thunderstorm motion. *Mon. Wea. Rev.,* **110,** 136-151.

Scofield, R. A. and J. F. W. Purdom, 1986: The use of satellite data for mesoscale analyses and forecasting applications. *Mesometeorology and Forecasting*, P.S. Ray, Ed., Amer. Meteor. Soc., 793pp.

Stumpf, G. J., A. W. Witt, E. D. Mitchell, P. L. Spencer, J. T. Johnson, M. D. Eilts, K. W., Thomas, and D. W. Burgess, 1998: The National Severe Storms Laboratory. Mesocyclone Detection Algorithm for the WSR-88D. *Wea. Forecasting,* **13,** 304-326.

Trapp, R. J., G. J. Stumpf, and K. L. Manross, 2005: A reassessment of the percentage of tornadic mesocyclones. *Wea. Forecasting,* **20,** 680-687.

Weaver, J., J. F. W. Purdom, and K. J. Szoke, 1994: Some mesoscale aspects of the 6 June 1990 Limon, Colorado, tornado case. *Wea. Forecasting,* **9,** 45-61.

___ and ___, 1995: An interesting mesoscale storm-environment interaction observed just prior to changes in severe storm behavior. *Wea. Forecasting,* **10,** 449-453.

___, J. A. Knaff, D. Bikos, G. S. Wade, and J. M. Daniels, 2002: Satellite observations of a severe supercell thunderstorm on 24 July 2000 made during the *GOES-11* science test. *Wea. Forecasting,* **17,** 124-138.

___ and D. Lindsey, 2004: Some frequently overlooked severe thunderstorm characteristics observed on GOES imagery: A topic for future research. *Mon. Wea. Rev.,* **132,** 1529-1533.

Weckwerth, T. M., J. W. Wilson, and R. M. Wakimoto, 1996: Thermodynamic variability within the convective boundary layer due to horizontal convective rolls. *Mon. Wea. Rev.,* **124,** 769-784.

___, T. M., J. W. Wilson, R. M. Wakimoto, and N. A. Crook, 1997: Horizontal convective rolls: Determining the environmental conditions supporting their existence and characteristics. *Mon. Wea. Rev.,* **125,** 505-526.

___, T. W. Horst, and J. W. Wilson, 1999: An observational study of the evolution of horizontal convective rolls. *Mon. Wea. Rev.,* **127,** 2160-2179.

___, 2000: The effect of small-scale moisture variability on thunderstorm initiation. *Mon. Wea. Rev.,* **128,** 4017-4030.

Wilson, J. W., G. B. Foote, N. A. Crook, J. C. Fankhauser, C. G. Wade, J. D. Tuttle and C. K. Mueller, 1992: The role of boundary-layer convergence zones and horizontal convective rolls in the initiation of thunderstorms: A case study. *Mon. Wea. Rev.,* **120,** 1785-1815.

Witt, A., M. D. Eilts, G. J. Stumpf, E. D. Mitchell, J. T. Johnson, and K. W. Thomas, 1998: Evaluating the performance of WSR-88D severe storm detection algorithms. *Wea. Forecasting*, **13,** 513-518.

Wood, V. T., R. A. Brown, and D. W. Burgess, 1996: Duration and movement of mesocyclones associated with southern Great Plains thunderstorms. *Mon. Wea. Rev.,* **124,** 97-101.

9. Figure captions

Figure 1. Visible satellite imagery taken on 7 June 2005 at 2325 UTC, 2332 UTC, and 2340 UTC over SE South Dakota. White arrows denote the location of feeder clouds; black arrows refer to a developed area of horizontal convective roll (HCR) clouds.

Fig. 2. Schematic diagram of a supercell thunderstorm showing a plan view of (left) an idealized, base-reflectivity radar echo, the RFD and gust front (depicted by the cold front symbol) and (right) a satellite representation of the same storm showing feeder clouds in relation to the flanking line and anvil of a supercell thunderstorm. Taken from Weaver and Lindsey, (2004).

Fig. 3. GOES-12 1 km visible images (left) and base reflectivity from KTLX (right) of the supercell in central Oklahoma 8 May 2003. Feeder clouds are denoted by the cyan arrows and mesocyclone detections are denoted as the yellow circles. The white arrow denotes the region of the inflow notch and the yellow area points to the flanking line. The black arrows denote areas where horizontal convective rolls have formed.

Fig. 4. Classification of predictions for all three predictors of severe weather. Categories are defined by Table 3.

Figure 5. Summary of skill scores for all three predictors of severe weather. POD, FAR, and CSI are defined by Equations (1-3), respectively.
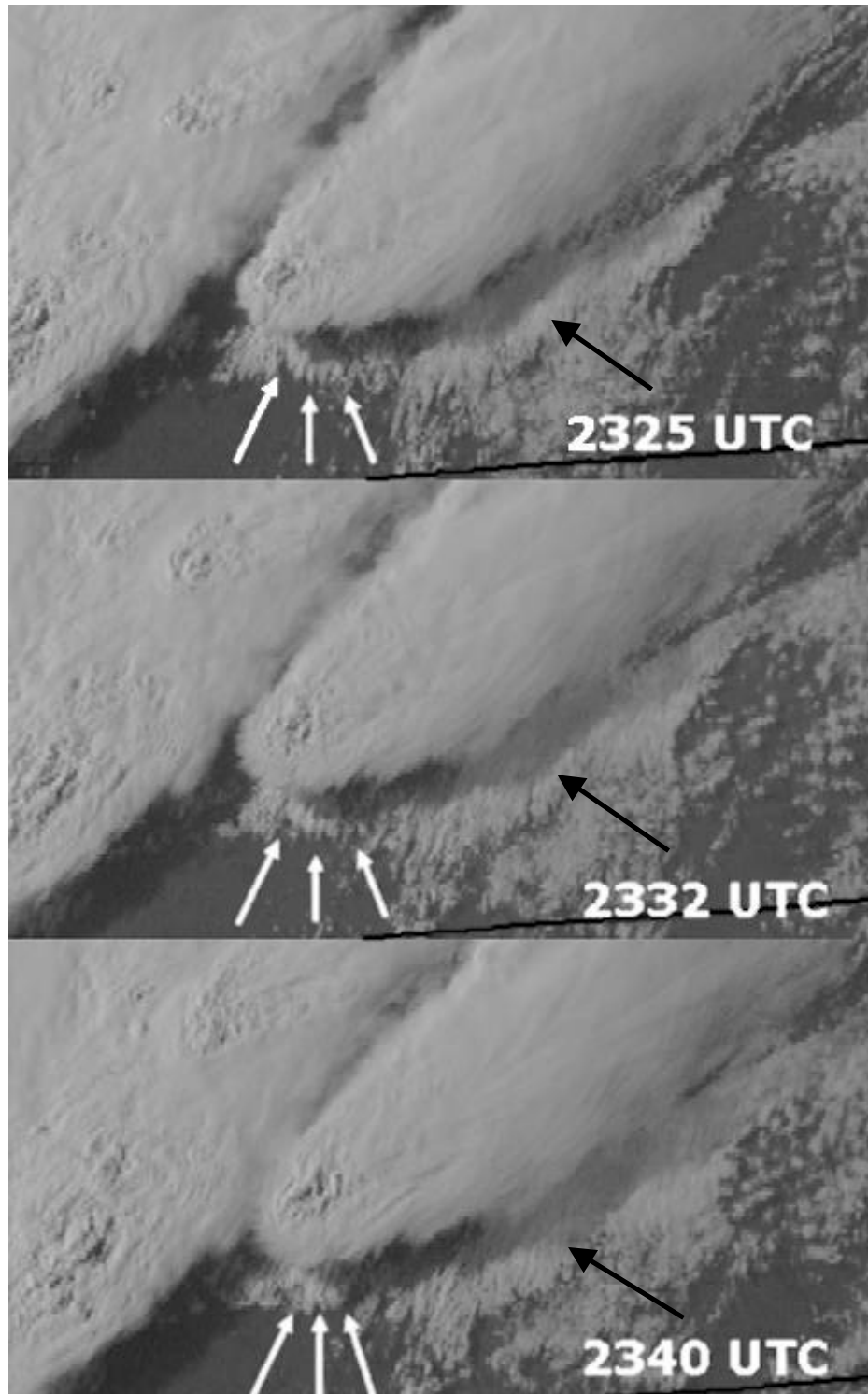
10. Figures and tables

Fig. 1. Visible satellite imagery taken on 7 June 2005 at 2325 UTC, 2332 UTC, and 2340 UTC over SE South Dakota. White arrows denote the location of feeder clouds; black arrows refer to a developed area of horizontal convective roll (HCR) clouds.
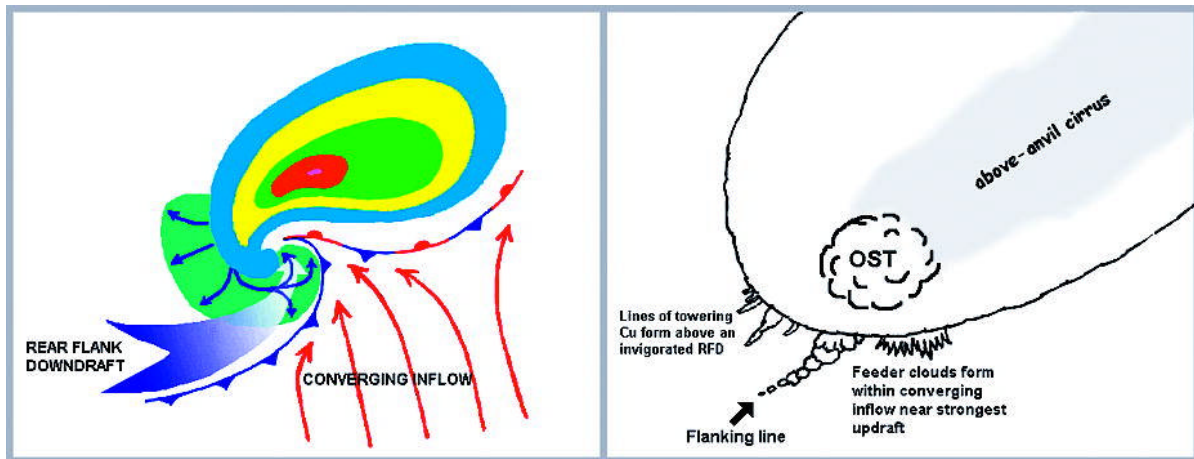
Fig. 2.   Schematic diagram of a supercell thunderstorm showing a plan view of (left) an idealized, base-reflectivity radar echo, the RFD and gust front (depicted by the cold front symbol) and (right) a satellite representation of the same storm showing feeder clouds in relation to the flanking line and anvil of a supercell thunderstorm. Taken from Weaver and Lindsey, (2004).
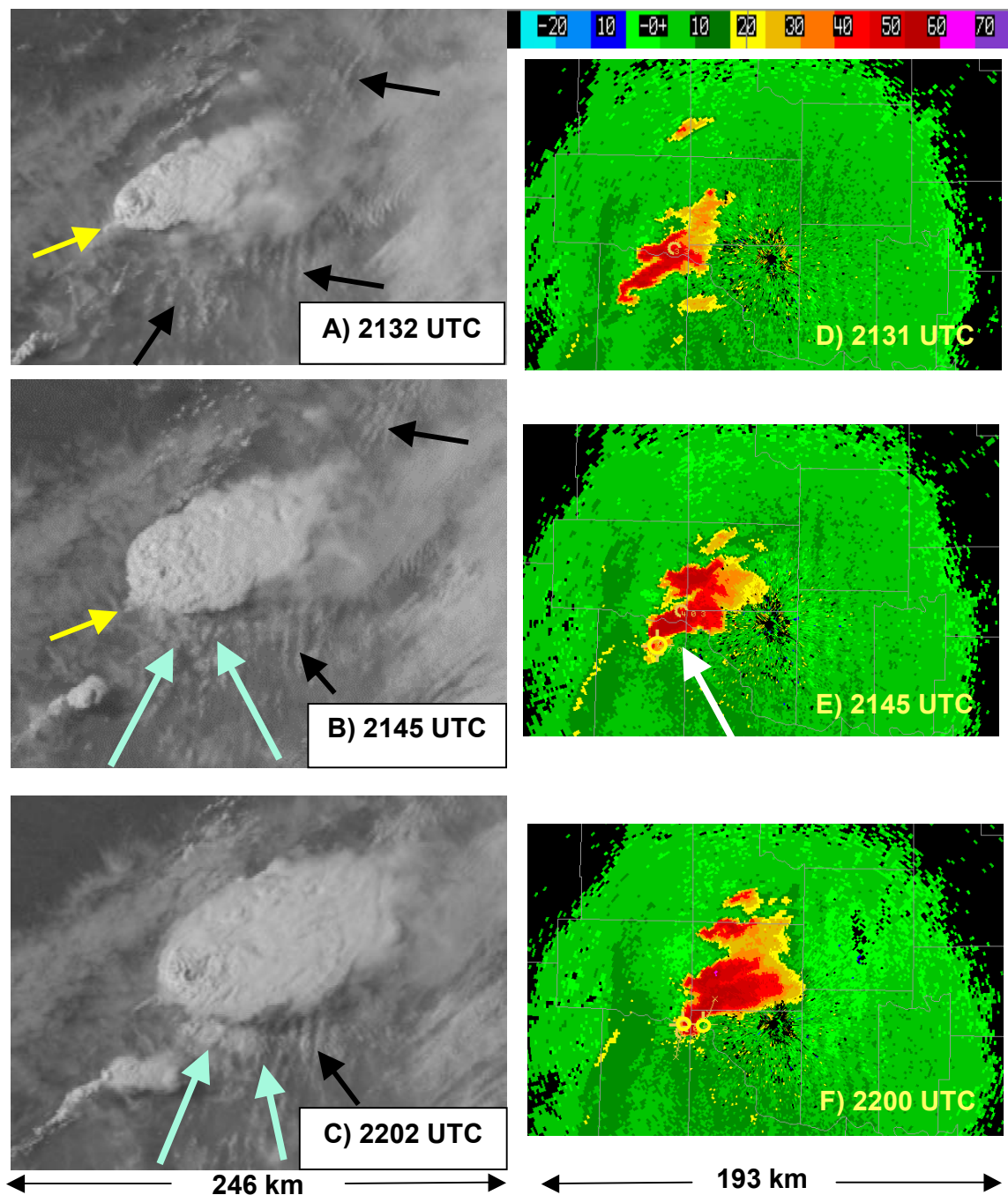
Fig. 3. GOES-12 1 km visible images (left) and base reflectivity from KTLX (right) of the supercell in central Oklahoma 8 May 2003. Feeder clouds are denoted by the cyan arrows and mesocyclone detections are denoted as the yellow circles. The white arrow denotes the region of the inflow notch and the yellow area points to the flanking line. The black arrows denote areas where horizontal convective rolls have formed.
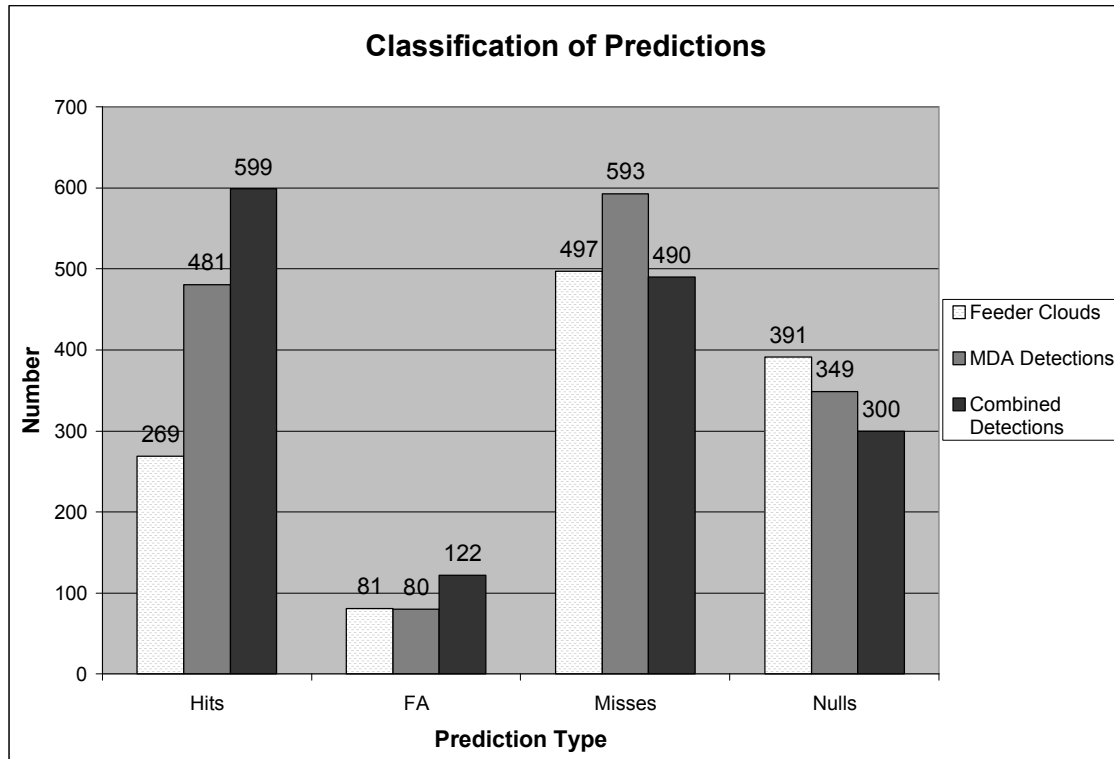
Fig. 4. Classification of predictions for all three predictors of severe weather. Categories are defined by Table 3.
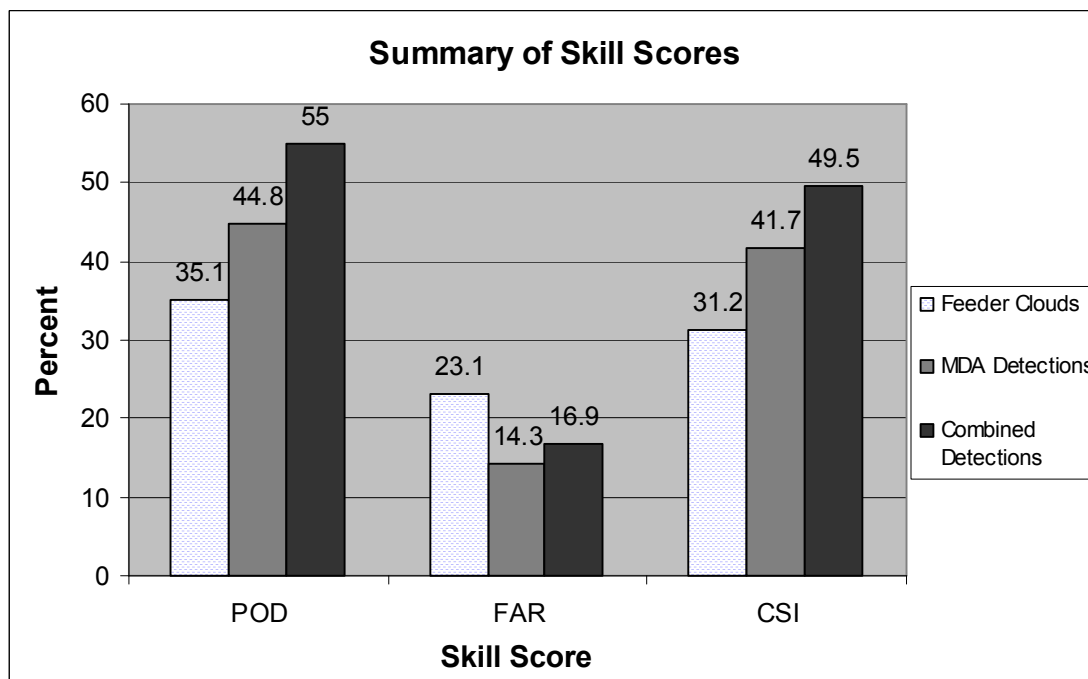

Fig. 5. Summary of skill scores for all three predictors of severe weather. POD, FAR, and CSI are defined by Equations (1-3), respectively.

TABLE 1. Severe weather case dates, number of thunderstorms, and thunderstorm locations

Date	Number of storms	Thunderstorm location by state
22-May-96	4	Nebraska, Wyoming, and Colorado
27-May-97	6	Texas, Louisiana, and Arkansas
16-Apr-98	6	Kentucky, Tennessee, and Mississippi
2-Jun-98	8	West Virginia, Pennsylvania, and New York
13-Jun-98	2	Nebraska and Kansas
21-Jan-99	5	Alabama, Georgia, Mississippi, and Louisiana
5-Jun-99	3	Nebraska and Kansas
13-Feb-00	3	Arkansas Louisiana
18-Apr-02	5	Iowa, Illinois, and Wisconsin
7-May-02	7	Texas, Oklahoma, and Kansas
19-Apr-03	4	Oklahoma and Texas
4-May-03	16	Oklahoma, Kansas, Nebraska, and South Dakota
8-May-03	9	Kansas, Nebraska, and Oklahoma
22-Jun-03	4	Wyoming, Nebraska, Kansas, and Iowa
24-Jun-03	9	South Dakota, Minnesota, Iowa, and Kansas
20-Apr-04	2	Illinois and Iowa
10-Jun-04	8	South Dakota, Nebraska, and Kansas
4-Aug-04	4	Oregon and Idaho
7-Jun-05	5	Wyoming and South Dakota
9-Jun-05	3	Nebraska, Kansas, and Oklahoma
27-Jun-05	3	Wyoming, Colorado, Kansas, Nebraska
9-Aug-05	4	Minnesota and Wisconsin
18-Aug-05	4	Wisconsin, Illinois, and Indiana
31-May-06	6	Colorado and Wyoming

TABLE 2. Severe weather case dates analyzed using radar imagery and number of thunderstorms

Date	Number of storms
16-Apr-98	6
2-Jun-98	3
5-Jun-99	2
18-Apr-02	5
7-May-02	7
19-Apr-03	4
4-May-03	12
8-May-03	9
22-Jun-03	3
24-Jun-03	9
10-Jun-04	8
4-Aug-04	4
7-Jun-05	5
9-Jun-05	3
27-Jun-05	3

TABLE 3. Contingency table template for various performance statistics

		Observed Event	
		Yes	**No**
Algorithm prediction	**Yes**	a. Hit	b. False Alarm (FA)
	No	c. Miss	d. Correct "No" Prediction (null)